NON-LINEAR THERMAL RADIATION AND MAGNETIC FIELD EFFECTS ON THE FLOW OF CARREAU NANOFLUID WITH CONVECTIVE CONDITIONS

by

Sajid QAYYUM[a*], Tasawar HAYAT[a,b], Ahmed ALSAEDI[b], and Bashir AHMAD[b]

[a] Department of Mathematics, Quaid-I-Azam University, Islamabad, Pakistan
[b] Non-linear Analysis and Applied Mathematics (NAAM) Research Group,
Faculty of Science, King Abdulaziz University, Jeddah, Saudi Arabia

Main features of the present analysis is to investigate the MHD non-linear mixed convection flow of Carreau nanofluid. Flow is due to stretching sheet with thermal and solutal convective conditions. Intention in present analysis is to develop a model for nanomaterial. The non-linear ordinary differential systems are obtained. Homotopy algorithm leads to solutions development. Velocity, temperature, nanoparticles concentration, surface drag force, and heat and mass transfer rate are displayed and argued. It is revealed that qualitative behaviors of velocity and layer thickness are reverse for material and magnetic parameters. Temperature field and heat transfer rate are similar observation for thermal Biot numbers. Moreover qualitative behaviors of nanoparticles concentration and mass transfer rate are reverse for larger Brownian motion.

Key words: *Carreau nanofluid, MHD, non-linear convection, non-linear thermal radiation, convective conditions*

Introduction

There are various fluids of industrial and engineering importance such as petroleum production, multigrade oils, polymers, composite material, shampoos, and fruit juices that show the viscoelastic aspects. Such fluids cannot be characterized simply like the Newtonian fluids. Because of the diversity of flow in nature, various non-Newtonian models have been recommended by the investigators [1, 2]. Among these models, Carreau fluid is one having importance in chemical engineering. Bird *et al.* [3] explained the detail of Carreau materials which are generally recognized as generalized Newtonian fluids. This model fits the performance of suspension of polymers in numerous fluid problems. It shows the viscous fluid purely where viscosity varies due to deformation rate. Ali and Hayat [4] discussed peristalsis of Carreau liquid in an asymmetric channel. Hayat *et al.* [5] analyzed the aspects of heat transfer in flow of Carreau fluid towards a stretched sheet. Hayat *et al.* [6] studied non-linear convective flow of Carreau nanofluid in the presence of Brownian motion and thermophoresis aspects. Hsiao [7] inspected MHD stagnation point flow of a Carreau nanoliquid towards a stretching surface. Features of Newtonian heating and MHD flow of Carreau liquid presented

---

[*] Corresponding author, e-mail: sajidqayyum94@gmail.com

by Hayat *et al.* [8]. The MHD flow of Carreau nanofluid with mass flux condition is investigated by Khan *et al.* [9]. Khan *et al.* [10] studied the radiative flow of Carreau nanofluid with heat generation/absorption.

The features of non-linear thermal radiation in boundary-layer flow is significant due to its application in industrial and engineering fields such as, furnace design, glass production, polymer processing, gas cooled nuclear reactors and also in space technology like aerodynamics rockets, propulsion system, missiles, power plants for inter planetary flights and space crafts which works at high temperatures. Consequently, thermal radiation effects cannot be ignored in such processes. The radiative heat flux in the energy equation is described through Rosseland relation. Cortell [11] examined the features of non-linear radiative flow of viscous fluid in the frame of stretched sheet. Hayat *et al.* [12] studied the mixed convection flow of tangent hyperbolic nanofluid with non-linear thermal radiation. An analysis for methanol and kerosene based ferrofluids flow with non-linear radiation is established by Reddy *et al.* [13]. Characteristics of non-linear thermal radiation and magnetic field flow of Sisko nanofluid has been studied by Soomro *et al.* [14]. Laxmi and Shankar [15] analyzed the radiative flow of viscous fluid in the frame of injection/suction. Some prominent literature for non-linear thermal radiation can be studied in the refs. [16-20].

Recent work has shown evidence that nanofluids are likely to have better thermal efficiency through the base fluids. Such fluids can be used in the procedures of vehicle computers, nuclear reactors, electronic cooling equipment, transportation and transformer cooling, heating and cooling process of energy conversion, cancer therapy, *etc.* Choi [21] provided an experimental work on nanofluid in view of various mechanisms. He concluded that the nanofluid is best suitable candidate for the betterment in heat transfer of ordinary liquids. Buongiorno [22] presented a detailed discussion on the effectiveness of nanoparticles in convective transport of ordinary fluids. Significance of CuO-water nanoparticles on surface of heat exchangers has been experimentally addressed by Pantzali *et al.* [23]. Hamad *et al.* [24] explain the laminar flow of viscous nanofluid in the frame of porous medium. The MHD flow of tangent-hyperbolic nanofluid towards a stretching sheet has been reported by Qayyum *et al.* [25]. Stagnation point flow of Jeffrey nanofluid with magnetic field has been investigated by Chakraborty [26]. Further relevant studies involving nanofluids can be seen through the investigations [27-30] and various studies therein.

The results obtained by homotopy analysis method (HAM) are preferred than the numerical solutions in perspective of the following points [31-39]:
- The HAM gives the solutions within the domain of interest at each point while the numerical solutions hold just for discrete points in the domain.
- Algebraically developed approximate solutions require less effort and having a sensible measure of precision when compared to numerical solution which are more convenient for the scientist, an engineer or an applied mathematician.
- Although most of the scientific packages required some initial approximations for the solution are not generally convergent. In such conditions approximate solutions can offer better initial guess that can be readily advanced to the exact numerical solution in the limited iterations. Finally an approximate solution, if it is analytical, is most pleasing than the numerical solutions.

Here our main emphasize is to visualize the non-linear mixed convection flow of Carreau nanofluid generated by movement of radiative sheet. Non-linear radiation term is incorporated in energy expression. Solutal and thermal convective conditions are considered. Aspects of MHD are analyzed in the mathematical modelling. The velocity, thermal field, nanoparticle

concentration, surface drag force and heat and mass transfer rate are graphically sketched and analyzed for various physical parameters.

Mathematical description

Let us investigate 2-D non-linear mixed convection flow of Carreau nanofluid past a stretched sheet at $y = 0$. Flow restricted is in the domain $y > 0$. Stretching surface has velocity $u_w(x) = ax$ (where a is the dimensional constant). A magnetic field of strength, B_0, is parallel in the y-direction. Induced magnetic field is absent for small magnetic Reynolds number. Non-linear thermal radiation, Brownian motion, and thermophoresis aspects are retained. Solutal and thermal convective conditions are imposed. Flow equations of Carreau nanofluid subject to usual boundary-layer approximations give:

$$\frac{\partial u}{\partial x} + \frac{\partial v}{\partial y} = 0 \tag{1}$$

$$u\frac{\partial u}{\partial x} + v\frac{\partial u}{\partial y} = \nu\frac{\partial^2 u}{\partial y^2}\left[1 + \left(\frac{n-1}{2}\right)\lambda^{*2}\left(\frac{\partial u}{\partial y}\right)^2\right] -$$

$$-\frac{\sigma B_0^2}{\rho}u + \nu(n-1)\lambda^{*2}\left[\frac{\partial^2 u}{\partial y^2}\left(\frac{\partial u}{\partial y}\right)^2\right]\left[1 + \left(\frac{n-3}{2}\right)\lambda^{*2}\left(\frac{\partial u}{\partial y}\right)^2\right] +$$

$$+ \mathrm{g}\{A_1(T - T_\infty) + A_2(T - T_\infty)^2\} + \mathrm{g}\{A_3(C - C_\infty) + A_4(C - C_\infty)^2\} \tag{2}$$

$$u\frac{\partial T}{\partial x} + v\frac{\partial T}{\partial y} = \frac{k_f}{(\rho c_p)_f}\left(\frac{\partial^2 T}{\partial y^2}\right) + \tau D_B\left(\frac{\partial T}{\partial y}\frac{\partial C}{\partial y}\right) + \frac{\tau D_T}{T_\infty}\left(\frac{\partial T}{\partial y}\right)^2 - \frac{1}{(\rho c_p)_f}\frac{\partial q_r}{\partial y} \tag{3}$$

$$u\frac{\partial C}{\partial x} + v\frac{\partial C}{\partial y} = D_B\left(\frac{\partial^2 C}{\partial y^2}\right) + \frac{D_T}{T_\infty}\left(\frac{\partial^2 T}{\partial y^2}\right) \tag{4}$$

with related boundary conditions are:

$$u = u_w(x) = ax, \quad v = 0, \quad -k\frac{\partial T}{\partial y} = h_t(T_f - T), \quad -D_B\frac{\partial C}{\partial y} = h_c(C_f - C) \text{ at } y = 0$$

$$u \to 0, \quad T \to T_\infty, \quad C \to C_\infty \text{ as } y \to \infty \tag{5}$$

where u and v are velocity components corresponding to x- and y-directions, respectively, $\nu = (\mu/\rho)_f$ – the kinematic viscosity, λ^* – the time constant, σ – the electrical conductivity, A_1 and A_2 – the linear and non-linear thermal expansions coefficients, A_3 and A_4 – the linear and non-linear concentration expansion coefficients, ρ_f and ρ_p – the fluid and particle densities, $(c_p)_f$ and $(c_p)_p$ – the fluid and particle heat capacities, k_f – the thermal conductivity, q_r – the radiative heat flux, $\tau = (\rho c_p)_p/(\rho c_p)_f$ – the capacity ratio, D_B and D_T – the Brownian and themophoresis diffusion coefficients, T and C – the fluid temperature and concentration, T_∞ and C_∞ – the ambient fluid temperature and nanoparticle concentration, n – the power law index, h_t and h_c – the coefficient of heat and mass transfer.

By Rosseland approximation, radiative heat flux q_r is:

$$q_r = -\frac{4\sigma^*}{3k^*}\frac{\partial T^4}{\partial y} = -\frac{16\sigma^*}{3k^*}T^3\frac{\partial T}{\partial y} \tag{6}$$

where σ^* and k^* present the Stefan-Boltzmann constant and the Rosseland mean absorption coefficient, respectively. Now eqs. (3) and (6) yield:

$$u\frac{\partial T}{\partial x} + v\frac{\partial T}{\partial y} = \frac{k_f}{\left(\rho c_p\right)_f}\frac{\partial^2 T}{\partial y^2} + \tau D_B\left(\frac{\partial T}{\partial y}\frac{\partial C}{\partial y}\right) + \frac{\tau D_T}{T_\infty}\left(\frac{\partial T}{\partial y}\right)^2 +$$

$$+\frac{1}{\left(\rho c_p\right)_f}\frac{16\sigma^*}{3k^*}\frac{\partial}{\partial y}\left(T^3\frac{\partial T}{\partial y}\right) \tag{7}$$

By using the similarity variables:

$$\eta = \sqrt{\frac{a}{v}}y, \quad \theta(\eta) = \frac{T-T_\infty}{T_f-T_\infty} \text{ or } T = T_\infty\left[1+(\theta_w-1)\theta\right], \quad \phi(\eta) = \frac{C-C_\infty}{C_f-C_\infty}, \tag{8}$$

$$u = axf'(\eta), \quad v = -\sqrt{av}f(\eta), \quad \psi(\eta) = \sqrt{av}xf(\eta)$$

Equation (1) is trivially satisfied and other equations yield:

$$f'''\left[1+\left(\frac{n-1}{2}\right)\alpha f''^2\right] + 2\left[\left(\frac{n-1}{2}\right)\alpha f''^2\right]\left[1+\left(\frac{n-3}{2}\right)\alpha f''^2\right] +$$

$$+ff'' - f'^2 - Ha^2 f' + \lambda(1+\beta_t\theta)\theta + \lambda N^*(1+\beta_c\phi)\phi = 0 \tag{9}$$

$$\left(1+\frac{4}{3}R\right)\theta'' + \frac{4}{3}R\left\{(\theta_w-1)^3\left[3\theta^2\left(\theta'\right)^2 + \theta^3\theta''\right] + 3(\theta_w-1)^2\left[2\theta\left(\theta'\right)^2 + \theta^2\theta''\right] +\right.$$

$$\left.+3(\theta_w-1)\left[\left(\theta'\right)^2 + \theta\theta''\right]\right\} + \Pr f\theta' + \Pr Nb\,\theta'\phi' + \Pr Nt\left(\theta'\right)^2 = 0 \tag{10}$$

$$\phi'' + \mathrm{Sc}f\phi' + \frac{Nt}{Nb}\theta'' = 0 \tag{11}$$

$$f'(\eta) = 1, f(\eta) = 0, \quad \theta'(\eta) = -B_t[1+\theta(\eta)], \quad \phi'(\eta) = -B_c[1+\phi(\eta)] \text{ at } \eta = 0$$

$$f'(\eta) = 0, \quad \theta(\eta) = 0, \quad \phi(\eta) = 0 \text{ as } \eta \to \infty \tag{12}$$

where α is the material variable, Ha – the magnetic parameter/Hartman number, λ – the mixed convection variable, β_t and β_c for non-linear convection variable due to temperature and concentration, N^* – the concentration thermal buoyancy forces ratio, R – the radiation parameter, θ_w – the temperature variable, Pr – the Prandtl number, Nb – the for Brownian motion variable, Nt – the thermophoresis variable, Sc – the Schmidt number, Gr and Gr* – the Grashof number in terms of temperature and concentration and B_t and B_c for Biot numbers in view of heat and mass transfer. Definitions of these variables are:

$$\alpha = \lambda^{*2}a^2, \ \mathrm{Ha} = \frac{\sigma B_0^2}{\rho a}, \ \lambda = \frac{\mathrm{Gr}}{\mathrm{Re}_x^2}, \ \beta_t = \frac{\varLambda_2(T_f-T_\infty)}{\varLambda_1}, \ N^* = \frac{\mathrm{Gr}^*}{\mathrm{Gr}} = \frac{\varLambda_3\left(C_f-C_\infty\right)}{\varLambda_1\left(T_f-T_\infty\right)}$$

$$\beta_c = \frac{\varLambda_4\left(C_f-C_\infty\right)}{\varLambda_3}, \ R = \frac{4\sigma^*T_\infty^3}{k_f k^*}, \ \theta_w = \frac{T_f}{T_\infty}, \ \Pr = \frac{\mu c_p}{k_f}, \ Nb = \frac{\tau D_B\left(C_f-C_\infty\right)}{v}$$

$$Nt = \frac{\tau D_T\left(T_f-T_\infty\right)}{vT_\infty}, \ \mathrm{Sc} = \frac{v}{D_B}, \ B_t = \frac{h_t}{k}\sqrt{\frac{v}{a}}, \ B_c = \frac{h_c}{D_B}\sqrt{\frac{v}{a}}, \ \mathrm{Gr} = \frac{g\varLambda_1\left(T_f-T_\infty\right)x^3}{v^2}$$

$$\mathrm{Gr}^* = \frac{g\varLambda_3(C_f-C_\infty)x^3}{v^2} \tag{13}$$

Qayyum, S., *et al.*: Non-Linear Thermal Radiation and Magnetic Field Effects ...
THERMAL SCIENCE: Year 2020, Vol. 24, No. 2B, pp. 1217-1228

1221

Physical quantities

The surface drag force, C_{fx}, heat transfer rate, Nu_x, and mass transfer rate, Sh_x, are interpreted:

$$C_{f_x} = \frac{\tau_w}{\frac{1}{2}\rho u_w^2}, \quad Nu_x = \frac{xq_w}{k_f(T_f - T_\infty)}, \quad Sh_x = \frac{xj_w}{D_B(C_f - C_\infty)} \tag{14}$$

in which τ_w, q_w, and j_w denote the surface shear stress and the surface heat and mass fluxes, respectively:

$$\tau_w = \eta_0 \left[\left(\frac{\partial u}{\partial y}\right) + \lambda^{*2}\left(\frac{n-1}{2}\right)\left\{ \frac{\partial u}{\partial y}\left(\frac{\partial u}{\partial x}\right)^2 + 3\frac{\partial v}{\partial x}\left(\frac{\partial u}{\partial y}\right)^2 \right\} \right]_{y=0}$$

$$q_w = -k_f \left(1 + \frac{4}{3}\frac{4\sigma^* T_\infty^3}{k_f k^*}\right)\left(\frac{\partial T}{\partial y}\right)_{y=0}, \quad j_w = -D_B\left(\frac{\partial C}{\partial y}\right) \tag{15}$$

In dimensionless form these quantities are expressed:

$$\frac{1}{2}Re_x^{0.5}C_{f_x} = \left[1 + \alpha\left(\frac{n-1}{2}\right)\right]f''(0), \quad Re_x^{-0.5}Nu_x = -\left\{1 + \frac{4}{3}R[1 + (\theta_w - 1)\theta(0)]^3\right\}\theta'(0)$$

$$Re_x^{-0.5}Sh_x = -\phi'(0) \tag{16}$$

where $Re = u_w x/\nu$ present local Reynolds number.

Homotopy analysis solutions

We choose the initial guesses $f_0(\eta)$, $\theta_0(\eta)$, and $\phi_0(\eta)$ linear operators $\mathbf{L}_f$, $\mathbf{L}_\theta$, and $\mathbf{L}_\phi$ for the velocity, temperature and concentration are expressed in the forms:

$$f_0(\eta) = 1 - \exp(-\eta), \quad \theta_0(\eta) = \frac{B_t}{1+B_t}\exp(-\eta), \quad \phi_0(\eta) = \frac{B_c}{1+B_c}\exp(-\eta) \tag{17}$$

$$\mathbf{L}_f(f) = \frac{d^3 f}{d\eta^3} - \frac{df}{d\eta}, \quad \mathbf{L}_\theta(\theta) = \frac{d^2\theta}{d\eta^2} - \theta, \quad \mathbf{L}_\phi(\phi) = \frac{d^2\phi}{d\eta^2} - \phi \tag{18}$$

with the properties:

$$\mathbf{L}_f\left[\Gamma_1 + \Gamma_2\exp(-\eta) + \Gamma_3\exp(\eta)\right] = 0$$
$$\mathbf{L}_\theta\left[\Gamma_4\exp(-\eta) + \Gamma_5\exp(\eta)\right] = 0 \tag{19}$$
$$\mathbf{L}_\phi\left[\Gamma_6\exp(-\eta) + \Gamma_7\exp(\eta)\right] = 0$$

We obtain the general solutions $f_m(\eta)$, $\theta_m(\eta)$, and $\phi_m(\eta)$ through the following procedure of refs. [25, 37-39]:

$$f_m(\eta) = f_m^*(\eta) + \Gamma_1 + \Gamma_2\exp(-\eta) + \Gamma_3\exp(\eta)$$
$$\theta_m(\eta) = \theta_m^*(\eta) + \Gamma_4\exp(-\eta) + \Gamma_5\exp(\eta) \tag{20}$$
$$\phi_m(\eta) = \phi_m^*(\eta) + \Gamma_6\exp(-\eta) + \Gamma_7\exp(\eta)$$

in which $f_m^*(\eta)$, $\theta_m^*(\eta)$, and $\phi_m^*(\eta)$ denote the special functions and Γ_i ($i = 1$-7) are the arbitrary constants given:

1222

Qayyum, S., *et al.*: Non-Linear Thermal Radiation and Magnetic Field Effects ...
THERMAL SCIENCE: Year 2020, Vol. 24, No. 2B pp. 1217-1228

$$\Gamma_1 = -\left.\frac{\partial f_m^*(\eta)}{\partial \eta}\right|_{\eta=0} - f_m^*(0), \quad \Gamma_2 = \left.\frac{\partial f_m^*(\eta)}{\partial \eta}\right|_{\eta=0}, \quad \Gamma_3 = 0$$

$$\Gamma_4 = \frac{1}{1+B_t}\left[\left.\frac{\partial \theta_m^*(\eta)}{\partial \eta}\right|_{\eta=0} - B_t \theta_m^*(0)\right], \quad \Gamma_5 = 0 \tag{21}$$
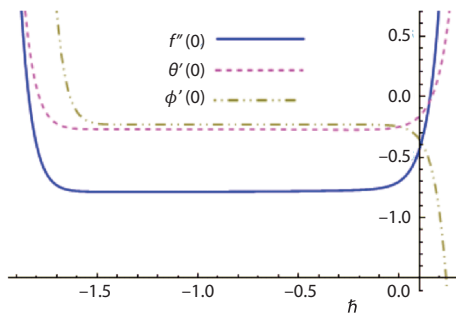
$$\Gamma_6 = \frac{1}{1+B_c}\left[\left.\frac{\partial \phi_m^*(\eta)}{\partial \eta}\right|_{\eta=0} - B_c \phi_m^*(0)\right], \quad \Gamma_7 = 0$$

Convergence of the homotopy solutions

The HAM contains auxiliary variables $\hbar_f$, $\hbar_\theta$, and $\hbar_\phi$. These auxiliary variables are efficient in adjusting and controlling the convergence. To obtain valid ranges of these variables, the $\hbar$-curves are sketched at 20th-order of approximations (see fig. 1). By looking at the range of variables the decisive values of $\hbar_f$, $\hbar_\theta$, and $\hbar_\phi$ are $-1.55 \leq \hbar_f \leq -0.15$, and $-1.60 \leq \hbar_\theta \leq -0.1$, and $-1.45 \leq \hbar_\phi \leq -0.15$

Table 1 is analyzed for convergence of the homotopic solutions. Here we observed that convergence for velocity is achieved 10th order of approximations and temperature and nanoparticles concentration is achieved at 6th order of approximations.

Figure 1. The $\hbar$-curves for $f''(0)$, $\theta'(0)$, and $\phi'(0)$

Table 1. Convergence solutions when $n = 2.0$, $\alpha = 2.0$, Ha = 0.1, $\lambda = 0.1$, $\beta_t = 0.1$, $N^* = 0.5$, $\beta_c = 0.1$, $R = 0.3$, $\theta_w = 1.1$, Pr = 2.0, $Nb = 0.2$, $Nt = 0.1$, Sc = 2.0, $B_t = 0.2$, and $B_c = 0.2$

Order of approximation	$-f''(0)$	$\theta'(0)$	$-\phi'(0)$
1	0.9513	0.1601	0.1602
5	0.9220	0.1549	0.1602
6	0.9210	0.1548	0.1555
10	0.9197	0.1548	0.1555
15	0.9197	0.1548	0.1555
20	0.9197	0.1548	0.1555
25	0.9197	0.1548	0.1555

Graphical results

The features of various physical quantities for velocity, temperature, nanoparticles concentration, surface drag force and heat and mass transfer rate are scrutinized through graphs. The used values of the quantities here are $n = 2.0$, $\alpha = 2.0$, Ha = 0.1, $\lambda = 0.1$, $\beta_t = 0.1$, $N^* = 0.5$, $\beta_c = 0.1$, $R = 0.3$, $\theta_w = 1.1$, Pr = 2.0, $Nb = 0.2$, $Nt = 0.1$, Sc = 2.0, $B_t = 0.2$, and $B_c = 0.2$.

Qayyum, S., *et al*.: Non-Linear Thermal Radiation and Magnetic Field Effects ...
THERMAL SCIENCE: Year 2020, Vol. 24, No. 2B, pp. 1217-1228

1223

Velocity field

Characteristics of *n vs.* velocity is explored in fig. 2. Clearly velocity and layer thickness increases when *n* is enhanced. In fact higher values of *n* increase non-linearity of the surface and this helps to reduce the resistive force. Figure 3 addresses α aspects *vs.* velocity. It is noted that both velocity and layer thickness are increased via α. Explanation of Ha on velocity are described via fig. 4. Clearly velocity reduces with an increment in Hartmann number. It is because of the reason that Lorentz force acts as a retarding force. Such retarding force enhances the frictional resistance opposing the liquid motion in the momentum boundary-layer thickness. Velocity for λ is drawn in fig. 5. Both velocity and layer thickness are boosted for larger λ. In fact that larger λ give rise to more buoyancy force and so velocity and layer thickness are enhanced.
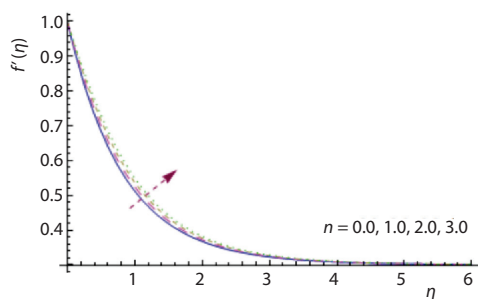
Figure 2. The $f'(\eta)$, via variation of *n*
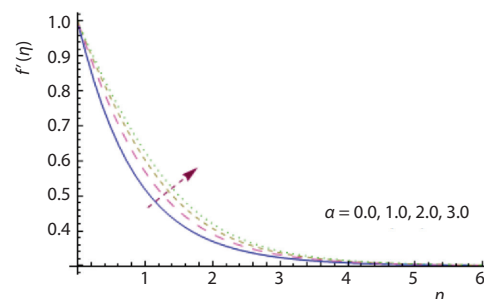
Figure 3. The $f'(\eta)$ via variation of α
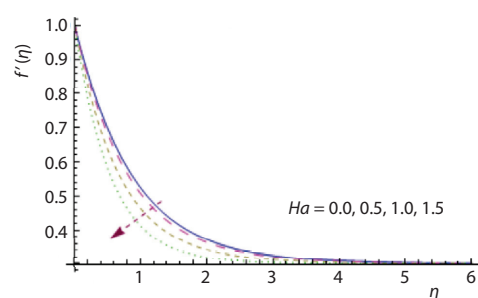
Figure 4. The $f'(\eta)$ via variation of Ha
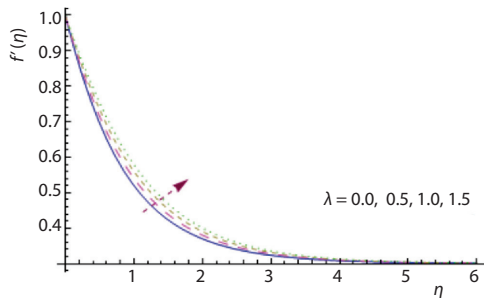

Figure 5. The $f'(\eta)$ via variation of λ

Temperature field

Figure 6 disclosed the behavior of *R*. Temperature field and layer thickness are increasing functions of *R*. As expected heat is produced due to radiation process in the working fluid so temperature field enhances. Figure 7 predicts the temperature field for θ_w. Both thermal field and related thickness layer boost when we increase values of θ_w (*i. e.*, temperature variable). Physically higher θ_w lead to an increase in convective surface temperature. Ultimate thermal field increases. Aspect of Prandtl number on temperature is described in fig. 8. Here both temperature and its layer thickness are reduced for larger Prandtl number. Physically higher Prandtl number lead to low thermal diffusivity which is responsible for temperature reduction. Figure 9 emphases temperature variation via *Nb*. For larger *Nb* both temperature and layer thickness

are increased. In fact more heat is produced through random motion of the fluid particles due to larger Brownian motion variable and consequently the temperature enhances. Temperature *vs.* Nt is disclosed in fig. 10. It is clear that both temperature and related layer thickness for larger Nt. In thermophoresis phenomenon heated particles are pulled away from hot surface to the cold region. Due to this fact the fluid temperature enhances. Figure 11 emphases on temperature *vs.* B_t. Obviously temperature and its related layer thickness have increasing function for B_t.
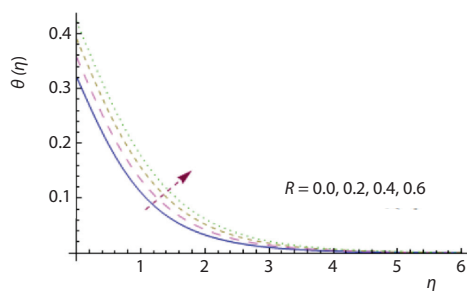
Figure 6. The $\theta(\eta)$ via variation of R
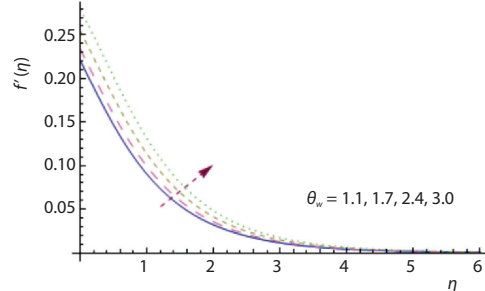
Figure 7. The $\theta(\eta)$ via variation of θ_w
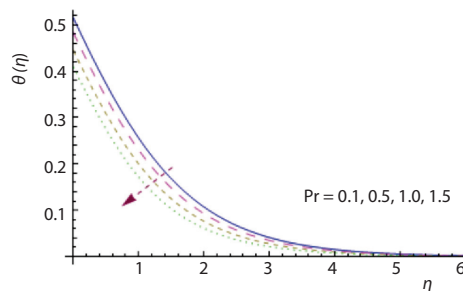
Figure 8. The $\theta(\eta)$ via variation of Pr
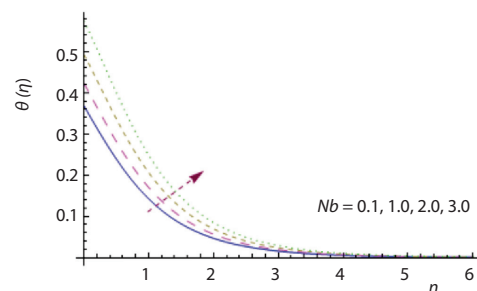

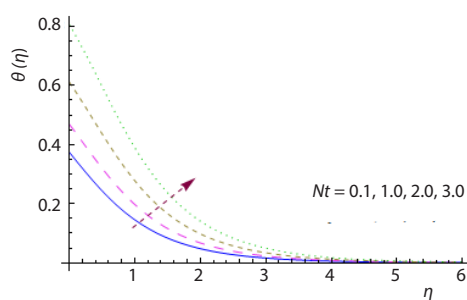**Figure 9. The $\theta(\eta)$ via variation of Nb**

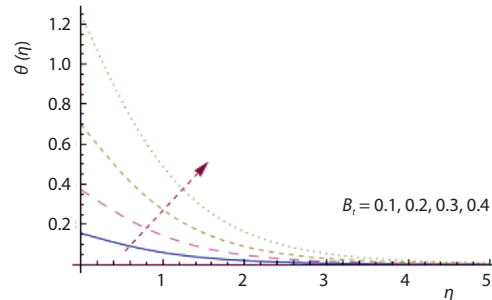**Figure 10. The $\theta(\eta)$ via variation of Nt**

Figure 11.The $\theta(\eta)$ via variation of B_t

Concentration field

Graphical illustration for concentration against Nb is captured in fig. 12. One may see from the figure that concentration is reduced via larger Nb. In fact Brownian motion appeared in the ratio form of nanoparticle mass species equation due to which the decreasing trend is noticed. Figure 13 witnesses that concentration field and thickness layer have increasing behavior

Qayyum, S., *et al.*: Non-Linear Thermal Radiation and Magnetic Field Effects ...
THERMAL SCIENCE: Year 2020, Vol. 24, No. 2B, pp. 1217-1228

1225

in the frame of Nt. Explanation of Schmidt number on concentration is demonstrated via fig. 14. Clearly concentration and layer thickness diminishes via larger Schmidt number. Since Schmidt number is relation of momentum and mass diffusivities. In fact for larger Schmidt number the mass diffusivity of the fluid decays which is responsible for reduction of concentration. Figure 15 emphases on B_c consequence against concentration. Both concentration and layer thickness are enhanced via larger B_c.
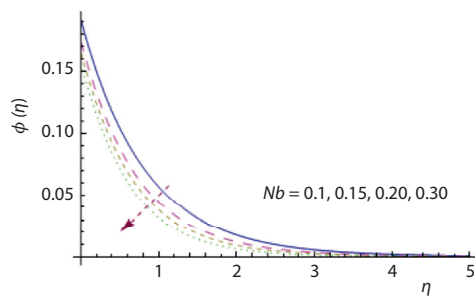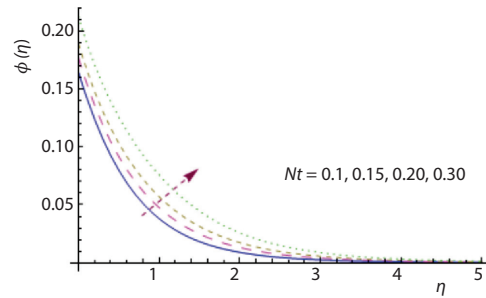
Figure 12. The $\phi(\eta)$ via variation of Nb
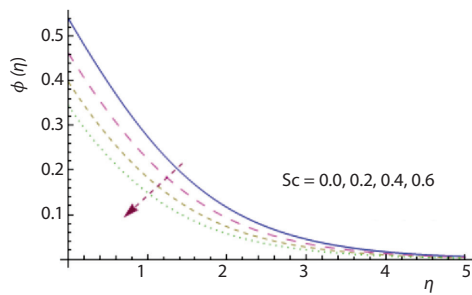
Figure 13. The $\phi(\eta)$ via variation of Nt

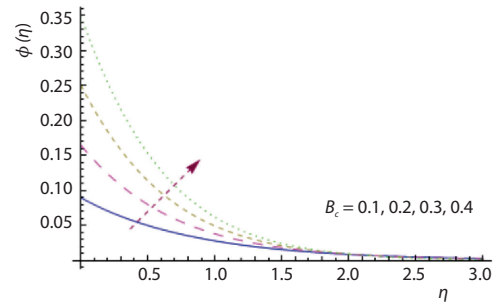**Figure 14. The $\phi(\eta)$ via variation of Sc**

Figure 15. The $\phi(\eta)$ via variation of B_c

Surface drag force

Features of α and Hartmann number on surface drag force are described in fig. 16. Here magnitude of surface drag force enhanced for larger α and Hartmann number. Figure 17 addresses n and λ behavior *vs.* surface drag force. It is clear that magnitude of surface drag force are reverse for n and λ.
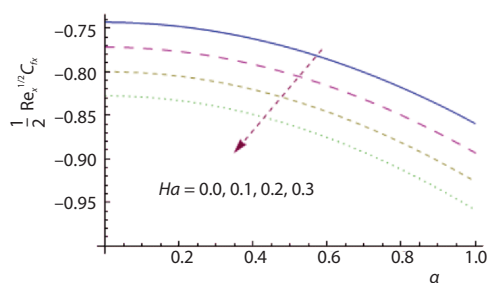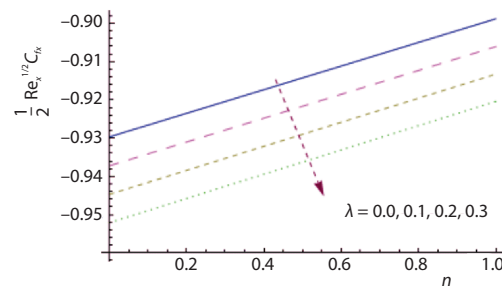
Figure 16. The $u_w(x) = ax$ via variations of α and Ha

Figure 17. The $1/2\mathrm{Re}_x^{1/2} C_{fx}$ via variations of n and λ

Heat transfer rate

Figure 18 interprets variations of heat transfer rate via B_t and Prandtl number. Here heat transfer rate is boosted when B_t and Prandtl number are increased. Aspects of heat transfer rate in the frame of Nb and Nt is disclosed in fig. 19. Clearly heat transfer rate decline when Nb and Nt are increased.
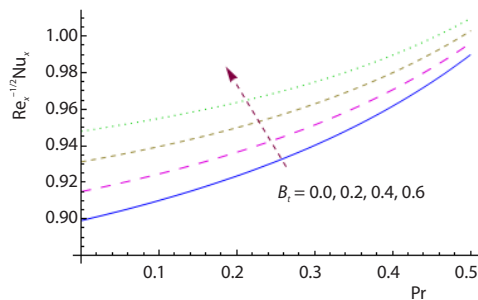
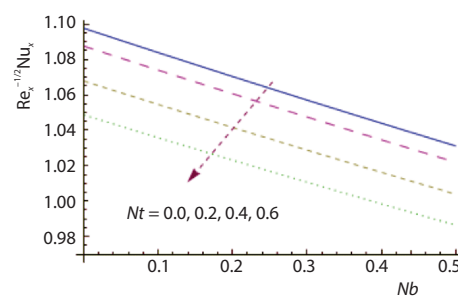**Figure 18. The $Re_x^{1/2}Nu_x$ via variations of Pr and B_t**

Figure 19. The $Re_x^{1/2}Nu_x$ via variations of Nb and Nt

Mass transfer rate

Aspects of Nb and Schmidt number, on mass transfer rate are explored in fig. 20. It is revealed that mass transfer rate enhances via Nb and Schmidt number. Figure 21 provides mass transfer rate via Nt and B_c. Mass transfer rate enhances via B_c while it decay in view of Nt.
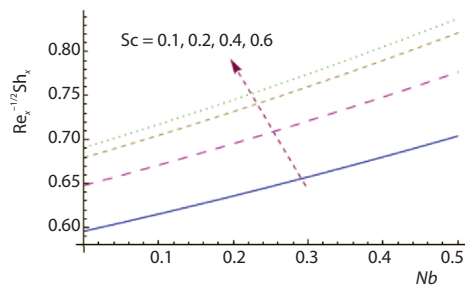
Figure 20. The $Re_x^{1/2}Sh_x$ via variations of Nb and Sc
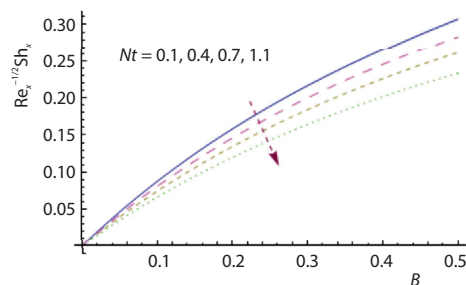
Figure 21. The $Re_x^{1/2}Sh_x$ via variations of B_c and Nt

Table 2. Comparison of skin friction coefficient for various values of Hartmann number with previous exiting results when $n = 1.0$, $\alpha = 0.0$, $\lambda = 0.0$, $\beta_t = 0.0$, $N^* = 0.0$, and $\beta_t = 0.0$

Ha	[28]	Present results
0.0	−1.00000	−1.00000
0.2	−1.01980	−1.01961
0.5	−1.11803	−1.11177
0.8	−1.28063	−1.28042
1.0	−1.41421	−1.41407

Qayyum, S., *et al.*: Non-Linear Thermal Radiation and Magnetic Field Effects ...
THERMAL SCIENCE: Year 2020, Vol. 24, No. 2B, pp. 1217-1228

1227

Comparative values of skin friction coefficient for the various values of Hartmann number with previous published work are examined in tab. 2. It is recognized that our results are in good agreement with the previous solutions in limiting cases.

Conclusions

The present study has following key points.
- Opposite behavior of velocity field is noticed in view of α and Hartmann number.
- Thermal field via θ_w and B_t has similar qualitative behavior.
- Concentration and related layer thickness for Nb and Nt have reverse effect.
- Magnitude of surface drag force are reverse for n and λ.
- Heat transfer rate is boosted when B_t and Prandtl number are increased.
- Larger Schmidt number retards concentration while reverse scenario is noted for mass transfer rate.

References

[1] Mousavi, S. M. R., *et al.*, Analytical Flow Study of a Conducting Maxwell Fluid through a Porous Saturated Channel at Various Wall Boundary Conditions, *Eur. Phys. J. Plus*, *129* (2014), Aug., 181
[2] Zaib, A., *et al.*, Dual Solutions of Non-Newtonian Casson Fluid-Flow and Heat Transfer over an Exponentially Permeable Shrinking Sheet with Viscous Dissipation, *Model. Simul. Eng.*, *2016* (2016), ID6968371
[3] Bird, R. B., *et al.*, *Dynamics of Polymeric Liquids,* Wiley, New York. USA, 1987
[4] Ali, N., Hayat, T., Peristaltic Motion of a Carreau Fluid in an Asymmetric Channel, *Appl. Math. Comput. 193* (2007), 2, pp. 535-552.
[5] Hayat, T., *et al.*, Boundary-Layer Flow of Carreau Fluid over a Convectively Heated Stretching Sheet, *Appl. Math. Comput.*, *246* (2014), Nov., pp. 12-22
[6] Hayat, T., *et al.*, Theoretical Aspects of Brownian Motion and Thermophoresis on Non-Linear Convective Flow of Magneto Carreau Nanofluid with Newtonian Conditions, Results Phys., *10* (2018), Sept., pp. 521-528
[7] Hsiao, K. L., To Promote Radiation Electrical MHD Activation Energy Thermal Extrusion Manufacturing System Efficiency by Using Carreau-Nanofluid with Parameters Control Method, *Energy*, *130* (2017), July, pp. 486-499
[8] Hayat, T., *et al.*, Radiative Flow of Carreau Liquid in Presence of Newtonian Heating and Chemical Reaction, *Results Phys.*, *7* (2017), Jan., pp. 715-722
[9] Khan, M., *et al.*, Numerical Assessment of Solar Energy Aspects on 3-D Magneto-Carreau Nanofluid: A Revised Proposed Relation, *Int. J. Hyd. Energy*, *42* (2017), 34, pp. 22054-22065
[10] Khan, M., *et al.*, Impact of Forced Convective Radiative Heat and Mass Transfer Mechanisms on 3-D Carreau Nanofluid: A Numerical Study, *Eur. Phys. J. Plus*, *132* (2017), Dec., 517
[11] Cortell, R., Fluid-Flow and Radiative Non-Linear Heat Transfer over Stretching Sheet, *Journal King Saud Univ. Sci.*, *26* (2013), 2, pp. 161-167
[12] Hayat, T., *et al.*, Non-Inear Thermal Radiation Aspects in Stagnation Point Flow of Tangent Hyperbolic Nanofluid with Double Diffusive Convection, *Journal Mol. Liq.*, *223* (2016), Nov., pp. 969-978
[13] Reddy, J. V. R., *et al.*, Impact of Non-Linear Radiation on 3-D Magnetohydrodynamic Flow of Methanol and Kerosene Based Ferrofluids with Temperature Dependent Viscosity, *Journal Mol. Liq.*, *236* (2017), June, pp. 93-100
[14] Soomro, F. A., *et al.*, Melting Heat Transfer Analysis of Sisko Fluid over a Moving Surface with Non-Linear Thermal Radiation Via Collocation Method, *Int. J. Heat Mass Transf.*, *126* (2018), Part A., pp. 1034-1042
[15] Laxmi, T. V., Shankar, B., Effect of Non-Linear Thermal Radiation on Boundary-Layer Flow of Viscous Fluid over Non-Linear Stretching Sheet with Injection/Suction, *Journal Appl. Math. Phys.*, *4* (2016), 2, pp. 307-319
[16] Hayat, T., *et al.*, Inclined Magnetic Field and Heat Source/Sink Aspects in Flow of Nanofluid with Non-Linear Thermal Radiation, *Int. J. Heat Mass Transf.*, *103* (2016), Dec., pp. 99-107
[17] Makinde, O. D., Animasaun, I. L., Thermophoresis and Brownian Motion Effects on MHD Bioconvection of Nanofluid with Non-Linear Thermal Radiation and Quartic Chemical Reaction Past an Upper Horizontal Surface of a Paraboloid of Revolution, *Journal Mol. Liq.*, *221* (2016), Sept., pp. 733-743

[18] Kumar, R., *et al.*, Rotating Frame Analysis of Radiating and Reacting Ferro-Nanofluid Considering Joule Heating and Viscous Dissipation, *Int. J. Heat Mass Transf.*, *120* (2018), May, pp. 540-551

[19] Qayyum, S., *et al.*, Chemical Reaction and Heat Generation/Absorption Aspects in MHD Non-Linear Convective Flow of Third Grade Nanofluid over a Non-Linear Stretching Sheet with Variable Thickness, *Results Phy.*, *7* (2017), pp. 2752-2761

[20] Hayat, T., *et al.*, Modern Aspects of Non-Linear Convection and Magnetic Field in Flow of Thixotropic Nanofluid over a Non-Linear Stretching Sheet with Variable Thickness, *Physica B: Cond. Matt.*, *537* (2018), May, pp. 267-276

[21] Choi, S. U. S., Enhancing Thermal Conductivity of Fluids with Nanoparticle, in: *Developments and Applications of Non-Newtonian Flows* (Eds. Siginer, D. A., Wang, H. P.), ASME, New York, USA, 1995, MD-vol. 231/FED-vol. 66, pp. 99-105

[22] Buongiorno, J., Convective Transport in Nanofluids, *Journal Heat Transfer-Trans. ASME*, *128* (2006), 3, pp. 240-250

[23] Pantzali, M. N., *et al.*, Investigating the Efficacy of Nanofluids as Coolants in Plate Heat Exchangers (PHE), *Chem. Eng. Sci.*, *64* (2009), 14, pp. 3290-3300

[24] Hamad, M. A., Pop, I., Scaling Transformations for Boundary-Layer Flow near the Stagnation-Point on a Heated Permeable Stretching Surface in a Porous Medium Saturated with a Nanofluid and Heat Generation/Absorption Effects, *Trans. Porous Medium*, *87* (2010), Dec., pp. 25-39

[25] Qayyum, S., *et al.*, Mixed Convection and Heat Generation/Absorption Aspects in MHD Flow of Tangent-Hyperbolic Nanoliquid with Newtonian Heat/Mass Transfer, *Rad. Phys. Chem.*, *144* (2018), Mar., pp. 396-404

[26] Chakraborty, T., *et al.,* Analytical Approach to a Jeffrey Nanofluid-Flow Towards a Stagnation Point Co-existing with Magnetic Field and Melting Heat Effects, *Journal Mol. Liq.*, *229* (2017), Mar., pp. 443-452

[27] Khan, M., *et al.*, Non-Linear Radiative Flow of 3-D Burgers Nanofluid with New Mass Flux Effect, *Int. J. Heat Mass Transf.*, *101* (2016), Oct., pp. 570-576

[28] Shehzad, S. A., *et al.*, Influence of Convective Heat and Mass Conditions in MHD Flow of Nanofluid, *Bull. Pol. Acad. Sci. Tech. Sci.*, *63* (2015), 2, pp. 465-474

[29] Khan, M., Khan, W. A., The MHD Boundary-Layer Flow of a Power-Law Nanofluid with New Mass Flux Condition, *AIP Advances*, *6* (2016), 2, 025211

[30] Khan, M., Khan, W. A., Steady Flow of Burgers' Nanofluid over a Stretching Surface with Heat Generation/Absorption, *Journal Braz. Soc. Mech. Sci. Eng.*, *38* (2016), Dec., pp. 2359-2367

[31] Liao, S., *Homotopy Analysis Method in Non-Linear Differential Equations*, Springer and Higher Education Press, New York, USA, 2012

[32] Hayat, T., *et al.*, Thermally Radiative Stagnation Point Flow of Maxwell Nanofluid Due to Unsteady Convectively Heated Stretched Surface, *Journal Mol. Liq.*, *224* (2016), Part A, pp. 801-810

[33] Sardanyes, J., *et al.*, Activation of Effector Immune Cells Promotes Tumor Stochastic Extinction: A Homotopy Analysis Approach, *Appl. Math. Comput.*, *252* (2015), Feb., pp. 484-495

[34] Qayyum, S., *et al.*, Effect of a Chemical Reaction on Magnetohydrodynamic (MHD) Stagnation Point Flow of Walters-B Nanofluid with Newtonian Heat and Mass Conditions, *Nuclear Eng. Tech.*, *49* (2017), 8, pp. 1636-1644

[35] Liu, Q. X., *et al.*, Asymptotic Limit Cycle of Fractional Van der Pol Oscillator by Homotopy Analysis Method and Memory-Free Principle, *Appl. Math. Model.*, *40* (2016), 4, pp. 3211-3220

[36] Aquino, A. I., Bo-ot, L. Ma.T., Multivalued Behavior for a Two-Level System Using Homotopy Analysis Method, *Physica A*, *443* (2016), C, pp. 358-371

[37] Qayyum, S., *et al.*, Magnetohydrodynamic (MHD) Non-Linear Convective Flow of Jeffrey Nanofluid over a Non-Linear Stretching Surface with Variable Thickness and Chemical Reaction, *Int. J. Mech. Sci. 134* (2017), Dec., pp. 306-314

[38] Qayyum, S., *et al.*, Simultaneous Effects of Melting Heat Transfer and Inclined Magnetic Field Flow of Tangent Hyperbolic Fluid over a Non-Linear Stretching Surface with Homogeneous-Heterogeneous Reactions, *Int. J. Mech. Sci.*, *133* (2017), Aug., pp. 1-10

[39] Hayat, T., *et al.*, Radiation Effects on the Mixed Convection Flow Induced by an Inclined Stretching Cylinder with Non-Uniform Heat Source/Sink, *PLoS ONE*, *12* (2017), Apr., e0175584